

*Transmitted with the  
letterhead 8/4/98  
9808060161 980804*

**Corrosion Products of Steels in High-Level Waste Management  
at the Proposed Yucca Mountain Repository**

**Tae M. Ahn and Bret W. Leslie**

**August 4, 1998**

**NUDOC Accession Number:**

**U. S. Nuclear Regulatory Commission  
Washington, DC 20555-0001, USA**

9808060163 980804  
PDR WASTE  
WM-11 PDR

*REC'D W/ETR DTD 9808060161 980804*

## ABSTRACT

This letter report evaluates materials to be emplaced at the proposed Yucca Mountain repository. A particular focus is on assessing the mass of corrosion products of steels, discussing qualitatively the effects of corrosion products on near-field environments. The sources of corrosion products include overpacks, basket materials, multipurpose canisters, pour canisters of high-level waste glass, and steel sets that may be used to support drift walls. A design summary of these sources is presented. Based on total uniform corrosion, most of these steels are likely to be corroded in 15,000 years and approximately  $(5.6 - 7.1) \times 10^5$  Metric Tons (MT) of iron oxide will be generated from the source steels. The corrosion products are expected to be incrustated under near-static conditions. However, unlike underground corrosion in soil, corrosion products may be sloughed off and colloids may be generated, with flowing or dripping groundwater. During the period in which corrosion of steel occurs, oxygen may be depleted in the near field. With pitting corrosion, it is unclear how much concentrated and acidic pit chemistry would affect the overall chemistry outside of the pits.

## CONTENTS

	Page
ABSTRACT	i
CONTENTS	ii
LIST OF FIGURES	iii
LIST OF TABLES	iv
1. INTRODUCTION	1
2. CURRENT DESIGN OF WASTE PACKAGES AND DRIFT SUPPORTS, AND PREDICTED NEAR-FIELD ENVIRONMENT	
2.1 Waste Package	2
2.2 Drift Supports	3
2.3 Near-Field Environment	3
3. CORROSION MODES AND CALCULATION OF THE AMOUNT OF CORROSION PRODUCTS	
3.1 Corrosion Modes	5
3.2 Calculation of the Amount of Corrosion Products	5
4. PROPERTIES OF CORROSION PRODUCTS AND ALTERATION OF NEAR-FIELD ENVIRONMENT	8
5. RECOMMENDATIONS	10
6. CONCLUSIONS	10
7. REFERENCES	28

## LIST OF FIGURES

	Page
<b>Figure 1. Waste Package Major Components</b>	
(1-a). Canistered Spent Fuel Waste Package	11
(1-b). High-Level Waste Glass Waste Package	12
(1-c). Uncanistered Spent Fuel Waste Package	13
<b>Figure 2. A Schematic of Basket Structure (1-a and 1-c)</b>	14
<b>Figure 3. A Schematic of Steel Sets used in the ESF Design Construction</b>	15
<b>Figure 4. Predicted Temperature and Relative Humidity of Waste Package Surface</b>	16
<b>Figure 5. Model Prediction of: (a) Aqueous General Corrosion; and (b) Humid General Corrosion in DOE TSPA-95</b>	17
<b>Figure 6. Potential-pH Diagrams for Iron and Water at Room Temperature</b>	18
<b>Figure 7. Corrosion of Buried Plain Carbon Steel after 14 Years of Exposure</b>	19
<b>Figure 8. Chemistry inside Pit: (a) 18Cr-12Ni-2Mo-Ti Stainless; and (b) Iron</b>	20

## LIST OF TABLES

	Page
<b>Table 1. Chemical Composition of Candidate Alloys for Overpack</b>	
<b>1.1 Outer Layer</b>	<b>21</b>
<b>1.2 Inner Layer</b>	<b>22</b>
<b>Table 2. Types of Stainless Steels to be Used for MPCs, Baskets, and Pour Canisters</b>	<b>23</b>
<b>Table 3. Penetration Depth of Carbon Steel by Uniform Corrosion at Various Times Using a Constant Passive Current Calculated Using EBSPAC</b>	<b>24</b>
<b>Table 4. Mass of Corrosion Products Generated as the Result of Complete Corrosion of Outer Overpacks</b>	<b>24</b>
<b>Table 5. Mass of Corrosion Products Generated as the Result of Complete Corrosion of MPCs</b>	<b>25</b>
<b>Table 6. Mass of Corrosion Products Generated as the Result of Complete Corrosion of Basket Plates</b>	<b>25</b>
<b>Table 7. Mass of Corrosion Products Generated as the Result of Complete Corrosion of Pour Canisters</b>	<b>26</b>
<b>Table 8. Mass of Corrosion Products Generated as the Result of Complete Corrosion of Steel Sets that could be Used as Drift Supports</b>	<b>26</b>
<b>Table 9. Pit Volume per Overpack with Various Pit Sizes and Pit Densities</b>	<b>27</b>

## **1. INTRODUCTION**

For the proposed high-level waste (HLW) repository of Yucca Mountain (YM), the near field is that portion of the mountain where both physical and chemical properties have been altered by the proposed repository construction, operations, and radioactive waste emplacement [Wilder, 1993a]. The "Evolution of the Near-Field Environment" (ENFE) is one of the Key Technical Issues (KTIs) in the NRC's HLW management program. The resolution of this KTI requires evaluation of the transient near-field environment, and determining its impact on total performance assessment (TPA) calculations of predicted repository system behavior.

Expected near-field environmental processes for the proposed YM repository were reviewed previously [Glassley, 1986; Murphy, 1991; Wilder, 1993a,b]. However, these evaluations did not consider a new waste package (WP) design involving thick (12 cm), multi-wall overpacks [TRW Environmental Safety Systems, Inc., 1996]. Among several new design features, the emplacement of a large amount of steel from thick overpacks could potentially significantly alter the near-field environmental conditions. Additional items made from steels to be used at the proposed YM repository are:

- (i) basket materials that use carbon steel and borated stainless steel to accommodate spent nuclear fuel (SF) assemblies;
- (ii) mutipurpose canisters (MPCs) composed of stainless steel for transportation and storage of SF;
- (iii) pour canisters composed of stainless steel for transportation and storage of HLW glass; and
- (iv) carbon steel sets that may be used to support drift walls

This topical letter report summarizes current information on steel that may be used at the proposed YM repository. It also presents estimates of the amount of corrosion products that could be produced as the result of complete corrosion of the various steel-containing componenets. Finally, the report discusses the potential impact of the corrosion products on the near-field environmental conditions and potential performance of the repository.

## **2. CURRENT DESIGN OF WASTE PACKAGES AND DRIFT SUPPORTS, AND PREDICTED NEAR-FIELD ENVIRONMENT**

### **2.1 Waste Package**

Several WP designs have been proposed by the Department of Energy (DOE) over the history of the YM repository program [TRW Environmental Safety Systems, Inc., 1996]. Of these designs, the canistered fuel design is considered the primary choice [TRW Environmental Safety Systems, Inc., 1996]. Figure 1 shows schematic diagrams of proposed example designs for robust waste packages of canistered spent fuel (1-a), HLW glass (1-b), and uncanistered spent fuel (1-c) [TRW Environmental Safety Systems, Inc., 1996]. The information provided in the schematic diagrams for the canistered spent fuel and HLW glass is used in this study to predict the amount of corrosion products that may be formed in the near-field environment. The design presented in Figure (1-c) is used to illustrate the basket structure. The canistered spent fuel design, either 21 pressurized water reactor (PWR) or 40 boiling water reactor (BWR) SF assemblies are contained in a 316L stainless steel cylindrical MPC (3.5 cm wall thickness) in which a fuel basket, made of borated stainless steel and carbon steel (0.5 to 1.0 cm thickness), provides criticality control and enhances heat transfer. However, it is unclear whether DOE would take credit for the MPC. HLW glass logs are contained primarily in the cylindrical pour canister (Figure 1-b) made of austenitic stainless steels that are either 0.34 or 0.95 cm thick.

The MPC and the pour canister are surrounded by a cylindrical inner overpack made of a corrosion-resistant alloy (2.5 cm wall thickness). In turn, this assemblage is then contained in a cylindrical outer overpack made of a corrosion-allowance material (10 cm wall thickness). Among candidate materials for the overpacks [McCoy, 1996], a list of high ranking materials is shown in Table 1. The outer layer is the primary source of iron, whereas the inner layer is based on nickel with iron as the minor alloying element. This study is concerned with the potential generation of corrosion products, thus only the outer layer of the overpack is considered in the analysis. Carbon or alloy steels in Table 1 are also expected to be used as part of basket materials and as steel sets to support drift walls. Table 2 shows the chemistry of stainless steels considered for MPCs, pour canisters, and part of basket materials.

The proposed length of the canistered spent fuel package is 568.2 cm and the diameter is 180.2 cm. This base case design is the main one used in the present analysis. Alternate designs include WPs for uncanistered fuel (no MPC, Figure 1-c) and small canistered fuel (12 PWR or 24 BWR SF Assemblies). The outer diameter of an MPC is 146 cm and the length is 500 cm as summarized by Sridhar, et al. [1994]. Figure 2 shows conceptual details of the basket plates made of borated stainless steel and carbon steel. The sizes of plates range from about 8 cm to 460 cm [TRW Environmental Safety Systems, Inc., 1996]. The pour canister has an outer diameter of 61 cm and a height of 300 cm [TRW Environmental Safety Systems, Inc., 1996].

In addition to the above steels, carbon steel guides are also used for encasing pour canisters in overpacks as supports [McCoy, 1996]. Also, iron shots are being considered for filler inside the overpacks.

## 2.2 Drift Supports

In order to meet retrievability requirements in current regulations for the HLW repository, the underground drifts will need to be stabilized. Stabilization of the current Exploratory Studies Facility (ESF) uses concrete inverts to line the floor, while steel sets are used to support the walls and ceiling of the tunnel where tunnel stability requires support. The current reference case for the repository would use pre-cast concrete liners for the entirety of tunnel support. This option would greatly reduce the use of steel. The alternate option is to emplace steel sets as the tunnel support system, as in the ESF. If this option is used, steel would be present in the form of: rebar in invert segments; steel sets, set hardware, and steel lagging; and rock bolts, bolt plates, channel, and welded wire fabric. Two types of steel sets are considered in the ESF design. Circular arcs support the tunnel walls circumferentially. Between these circular arcs on the surface of the tunnel, numerous steel bars reinforce the walls. These bars are aligned in a parallel or perpendicular manner to the steel arcs. Many of these bars are cross-linked with each other. Examples of the steel set are in Figure 3. Circular arcs and steel bars are about (1 -20) cm in dimensions [TRW Environmental Safety Systems, Inc., 1997].

The extrapolation of ESF data to the repository drifts would overestimate the total amount of steel that could be used in the repository. This is because the repository drift diameter is smaller than the ESF tunnel size and because the repository drift may use pre-cast concrete liners. Currently, as the base case, 105 emplacement drifts are considered to be excavated. Among them, 95 drifts are pre-cast concrete segments reinforced with steel fibers; 10 drifts would be cast emplacement concretes with steel reinforcements. Altogether about 15,000 MT steel is expected to remain in the repository after the repository closure (Nolting, 1997). However, if steel sets are emplaced as the tunnel support systems, as options, the amount of steel to be emplaced would be increased by an order of magnitude.

## 2.3 Near-Field Environment

Aqueous corrosion of metallic materials is expected to be caused by two different mechanisms, under the repository conditions at the proposed YM site. With the dripping of groundwater through the unsaturated rocks, the overpack surface can get wet. However, during the containment period, in the early time of waste emplacement, the expected temperature would be well above room temperature. Under a humid environment, it is more likely that corrosion will take place with moisture condensed on the overpack surface [Mohanty, et al., 1996]. The temperature and relative humidity (RH) are the primary environmental factors to determine the extent of the wetting of the metallic surface. Therefore, RH and temperature at the metal surface as functions of time are used to predict the conditions that affect the occurrence and rate of the metallic corrosion.

The chemical composition, pH, and oxygen concentration of the condensed pore groundwater in rocks are predicted by multi-phase, non-isothermal, and multi-dimensional mass transport modeling of the environment, where the evaporative effects produced by heat released by radioactive decay are considered. Figure 4 [Wilder, 1996] shows a typical temperature and RH profile of the WP surface. The computer code MULTIFLO can predict pH, chloride concentration, and oxygen concentration in

the near field [Lichtner and Seth, 1996]. These calculations to predict the chemistry on the waste package surface requires assuming the groundwater equilibrated with hostrocks drips on the overpack surface. In a humid environment, the condensed water on the overpack surface can range from pure water to a sodium chloride dominated solution. The sodium chloride solution is expected if salt deposits formed during prior drips of groundwater and subsequent evaporation interact with vapor condensing on the waste package surface [Mohanty, et al., 1996]. Because the chemistry of condensed water is not known, calculations of NRC Engineered Barrier Performance Assessment Code (EBSPAC) adopt to sample the chloride concentration and pH [Mohanty et al., 1996].

### **3. CORROSION MODES AND CALCULATION OF THE AMOUNT OF CORROSION PRODUCTS**

#### **3.1 Corrosion Modes**

The base case of corrosion processes is that adopted in EBSPAC [Mohanty, et al., 1996]. Below a critical value of RH, air oxidation of steel takes place as the dominant degradation process of the steel overpack. As a result of thermal embrittlement of the steel promoted by long-term exposure to temperatures above 150 C, the steel may fail mechanically. If the RH is higher than the critical value, (aqueous) corrosion of the steel overpack will occur.

The corrosion takes place uniformly and locally. The corrosion process at any given time depends on the corrosion potential and the critical potential required to initiate a particular localized corrosion process. After penetration of the outer overpack, electrical contact of the inner and outer overpacks promotes galvanic coupling (through the presence of an electrolyte path such as that provided by modified groundwater) if metallic contact always exists between both overpacks. The efficiency of galvanic coupling determines in part whether localized corrosion penetration of the inner overpack is possible. With efficient galvanic coupling, the inner overpack becomes protected against localized corrosion and the outer overpack corrodes by uniform galvanic corrosion or localized corrosion.

Although other processes of corrosion have been recognized as potential failure mechanisms, they are not considered in the current performance assessment codes [Mohanty, et al., 1996; TRW Environmental Safety Systems, Inc., 1995]. Those processes include microbial corrosion, stress corrosion cracking, and hydrogen embrittlement.

Most corrosion experiments to evaluate waste packages have been conducted at near-neutral pH in mild J-13 well water augmented in chloride concentration up to 1000 ppm [Sridhar, et al., 1995]. More recently, aggressive solutions of high chloride concentration and low pH have been considered in the tests. However, some appropriate data are available from literature for generic engineering applications in severe environments. For instance, data are available on the corrosion of carbon at low pH and varying chloride concentrations [Sridhar, et al., 1994].

#### **3.2 Calculation of the amount of Corrosion Products**

Calculations of corrosion kinetics for overpacks under time-varying repository conditions were undertaken extensively in DOE Total System Performance Assessment (TSPA)-95 [TRW Environmental Safety System Inc., 1995] and NRC EBSPAC [Mohanty, et al., 1996]. However, these calculations have been conducted only up to the period of initial pit penetration. As far as localized corrosion is concerned, the propagation such as continuous pit formation and lateral growth of pits has not been assessed. In addition, the long-term kinetics of even uniform corrosion have not been evaluated for MPCs, pour canisters, steel sets in bore hole, and basket materials. The uniform corrosion kinetics of passive alloys,  $2 \times 10^{-7}$  A/cm<sup>2</sup>, would be lower by about an order of magnitude than that of carbon steel,  $1 \times 10^{-6}$  A/cm<sup>2</sup> [Mohanty, et al., 1996].

Table 3 shows the penetration of carbon steel by uniform corrosion at various times. Using the passive current density adopted above, about 1 cm is penetrated in 1000 years, and there is complete penetration within 8,600 years. The constant passive current is considered as a base case in near neutral environments. This is in general agreement with DOE TSPA-95 calculations, as shown in Figure 5 [TRW Environmental Safety System, Inc., 1995]. The corrosion kinetics of the outer layer is likely to bound the corrosion kinetics of carbon steel basket and drift steel sets (if the types of ESF steels are used in drifts). They are carbon steel and are likely to be thinner (at most the same order of magnitude [McCoy, 1997]) than overpacks. For borated stainless steels (less than 1 cm thick) and pour canisters (less than 1 cm), Table 3 calculations also would bound the corrosion kinetics of these materials. For MPC (about 3.5 cm thick), however, the corrosion times would be longer than those in Table 3 by factors of 1.8 (15,000 corrosion time) respectively.

Table 4 predicts the total amount of corrosion products generated from the complete corrosion of the outer overpack. In this calculation, various oxides are considered for 11,000 containers of SF [Manteufel, et al., 1997] and HLW glass. The number of HLW glass containers is based on four canisters per container. There would be 13,362 pour canisters from Hanford, Idaho and Savannah River, and 300 pour canister from West Valley [TRW Environmental Safety System Inc., 1996]. Approximately,  $(3.57 - 4.53) \times 10^5$  MT of iron oxides (upon the total conversion of metal to oxide) will be produced. In the presence of a cement liner or invert, the groundwater chemistry would be altered to be a high pH solution. Under high pH conditions, the corrosion rates can be increased at well above room temperature. As shown later (see Section 4), this fast corrosion requires pH ranges above 14 and temperatures well above room temperature. It is not known whether such a high pH environment would occur or not at the proposed YM repository. Similarly, microbial corrosion has not been considered in calculating corrosion rates.

Tables (5 - 7) show the calculated total amount of corrosion products generated from the complete corrosion of MPCs, basket plates and pour canisters. For 11,000 MPC (the same number of SF containers), about  $(9.45 \times 10^4 - 1.20 \times 10^5)$  MT of iron oxide will be produced. From basket plates of carbon steel and borated stainless steel for 11,000 SF containers, about  $(1.03 - 1.30) \times 10^5$  MT of iron oxide will be produced. Finally, from pour canisters, about  $(7.95 \times 10^3 - 1.01 \times 10^4)$  MT of iron oxide will be produced.

Table 8 shows the calculated total amount of corrosion products from steel sets. In the calculation, approximately 15,000 MT steels are used for 105 emplacement drifts (Nolting, 1997). The resulting iron oxides from the used carbon steel will be about  $(2.07 - 2.63) \times 10^4$  MT. This value is less than that from overpacks. However, if steel sets as the tunnel support are used, as options, the amount of steel to be emplaced would be increased by an order of magnitude.

In addition to the above steels, carbon steel guides are also used for encasing pour canisters in overpacks as supports [McCoy, 1996]. The mass of the steel used in the guides would be much smaller than that used in other items described in Tables 4-8. Iron shots for filler are optional. If used, the amount of oxides could be slightly less than that from outer overpacks.

During localized corrosion, the chemistry inside pits is expected to be different from the outside ambient chemistry of any fluid. The pit chemistry would be highly acidic and concentrated with chloride by the formation of various salts such as ferric chloride [Szklaarska-Smialowska, 1986]. A summary of literature data shows that typical pit density is  $(0.1 - 100)/\text{cm}^2$  and pit size is  $(\mu\text{m} - \text{mm})$  in diameter [Ahn, 1994]. Table 9 shows a comparison of total volumes of overpack materials and pit

volume at selected values of pit density and pit size. As pit density is increased and pit diameter becomes bigger, the pit volume becomes comparable with the overpack volume and the container volume. The comparison of pit volume with the volume of near-field groundwater is very arbitrary, depending on the water contact mode of groundwater with waste packages and the amount of groundwater remained in the failed container. Under the immersion condition, the groundwater volume would be large, whereas only thin film of groundwater would be available under drip condition or as condensed water in the humid environment.

Nonetheless, it should be noted that literature data on pit density and pit diameter were mostly obtained at the stage of pit initiation. Data on severe pit propagation predict mostly the growth of pit depth rather than the lateral growth of pit diameter. When the lateral growth of many pits becomes severe, the volume of pits may be large, whereas the chemistry inside pits becomes less severe (see Section 4).

#### 4. PROPERTIES OF CORROSION PRODUCTS AND ALTERATION OF NEAR-FIELD ENVIRONMENT

Figure 6 shows potential-pH diagrams for the iron and water system at room temperature. In this figure, the oxide is shown to be thermodynamically unstable at high or low pH. At pH values closer to neutral, oxides become stable. Literature data also shows that corrosion rates would be increased kinetically at low (below about 2) and high (above about 14) pH, mostly at elevated temperatures [American Society for Metals, 1987]. In between these two extremes, corrosion rates will be decreased due to the onset of passivity. In this intermediate pH region, the formation of protective oxide film is favored.

A summary of investigations of oxides on mild steel in oxygenated water [Sridhar, et al., 1994] has shown that  $\gamma$ -FeOOH initially forms on the surface at room temperature. With time, this film is converted to a mixture of  $\gamma$ -FeOOH and  $\text{Fe}_3\text{O}_4$ . In addition,  $\text{Fe}(\text{OH})_2$  has also been reported to form under these conditions. Increasing the temperature to 50-100 C favors the formation of  $\text{Fe}_3\text{O}_4$ , since at temperatures around 100 C,  $\text{Fe}(\text{OH})_2$  decomposes to  $\text{Fe}_3\text{O}_4 + \text{H}_2$ . During the formation of these oxides,  $\text{Fe}^{+2}$  (reducing environments),  $\text{Fe}^{+3}$  (oxidizing environments), and  $\text{Fe}(\text{OH})^{+2}$  are present. Also, during air oxidation,  $\text{Fe}_2\text{O}_3$  is likely to form too. In the presence of microbes, corrosion rates may increase or decrease, depending on the type of microbes and other environmental conditions. Under anaerobic conditions, iron sulfides form on the surface of mild steel; under fluctuating aerobic and anaerobic conditions, various sulfides, ferric oxide and ferric oxyhydroxides form [Geesey, 1993]. During microbial corrosion, pH in the vicinity of biofilm is expected to be low, if organic acids such as oxalic or formic acid forms.

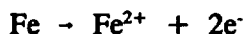
In the proposed YM environment, the amount of groundwater in contact with waste packages could be limited or near static. In addition, evaporation of water that contacts the waste packages would change stability limits depicted in Figure 6. Under these conditions, dissolved iron oxides may reach solubility limits in a wider range of pH value. Nonetheless, the corrosion products would be continuously produced, limited by the solubility of iron in groundwater. This is because metal corrodes electrochemically (i.e., irreversibly). However, the long-term corrosion rates would be decreased if the oxides formed retard mass transport significantly.

In a base case excluding solutions of very high or low pH values, solid oxides are formed as corrosion products. Although these corrosion products don't protect steels against further corrosion propagation, they remained in the vicinity of steel from literature data on underground corrosion. Romanoff conducted corrosion testings of various steels buried for longer than 10 years in soil [Romanoff, 1957]. The tested steel was incrustated with oxides. Corrosion products were not present at low pH, under flowing water or air, or under influence of microbes [Escalante, 1997]. Figure 7 is severely corroded steel and iron after removal of corrosion products. The steel and iron show large-sized and low-density pits. Jones reported similar examples [Jones, 1992]

However, there would be groundwater drips onto corrosion products under the repository condition. This is likely to erode corrosion products, especially associated with volume change upon oxidation [Ahn, 1996a]. The stress generated during oxidation is large enough to cause oxide spallation [Ahn, 1996b]. The erosion or spallation is one mechanism for the formation of colloids. This type of colloid

formation mechanism is called dispersion [Yariv and Cross, 1979]. For instance, Bates et al. conducted drip tests on  $\text{UO}_2$ , spent fuel, and HLW glass, and identified spalled oxide colloids transported from the surface [Finn, et al., 1994a,b; Bates, et al., 1992].

In a natural system, the potential pH diagram shown in Figure 6 can be regarded as an Eh-pH diagram. The corrosion of steel involves the anodic reaction of



and several cathodic reactions such as



Therefore, if oxygen is consumed, the Eh value will be lowered. Stockman [1997] postulates that oxygen will be depleted as the vapor phase drives out oxygen during the containment period and that oxygen will be consumed by the corrosion process after the containment period. However, the Eh will not be sufficiently low to destabilize iron oxide or to prohibit corrosion, as illustrated in Figure 6. The detailed evaluation of Stockman's model has not been conducted. Nonetheless, it is likely that corrosion products themselves limit oxygen supply for further corrosion of steel. In the absence of oxygen, steel will still corrode at lower rates with water.

Although most of the oxides form in crust, colloidal oxides may also form, particularly under flowing-water conditions or with the aid of microbes [Ahn, 1996a]. In natural groundwater systems, precipitated oxides and oxyhydroxides of Fe are common. Reactive surface area can be high for the amorphous forms of these minerals. For instance, synthetic  $\text{Fe}(\text{OH})_3$  has a surface area of about 150 to 800  $\text{m}^2/\text{g}$ . Dzombak and Morel [1990] suggest the potential importance of these minerals as a sorbent phase, especially for small particles like (suspensible) colloids. These colloids can carry highly sorptive actinides such as Pu. Sorption of Pu [Sanchez et al., 1985], Th [LaFlamme and Murray, 1987; Hunter, et al., 1988], and Np [Girvin, et al., 1991] on Fe oxyhydroxides shows sorption edges over a pH range from 3 to about 6, at the low end of the range ( $\sim 4$  to  $\sim 9$ ) reported in the vicinity of YM [U.S. Department of Energy, 1988]. However, cements will likely create hyperalkaline plumes and pH will be high. Under high pH conditions, sorption for most radioelements will decrease. Further, under the hyperalkaline conditions, colloids will agglomerate [Savage, 1997]. Currently, no data are available about what fraction of oxides or oxyhydroxides from corrosion can be colloids.

In the previous section, we have calculated total volume of pits compared with steel volume and container volume. It is not clearly understood that how much pit chemistry contributes to overall near-field chemistry. Figure 8 shows chloride concentrations versus pit diameters. Depending on materials and environmental conditions, there is a range of pit diameter carrying high-chloride salt solutions. If pit diameter becomes bigger than this size, pits would not carry high-chloride salt solutions. However, these values are averaged ones within pits. There would be longitudinal concentration gradient within a single pit. As pits become wider, mass transport within pit would be less limited. Consequently, severe chemistry would be localized near the bottom of pit, and eventually pit will stop to grow longitudinally upon further lateral growth of pit. This hypothesis implies that severe pit chemistry may affect the near-field chemistry, only if (a) pit diameter is sufficiently narrow, (b) groundwater outside of the pit is of thin film, and (c) limited mass transport within pit impose severe chemistry even near the mouth of pit.

## 5. RECOMMENDATIONS

For quantitative assessments of the near-field environment in the presence of corrosion products, the followings are recommended to be studied:

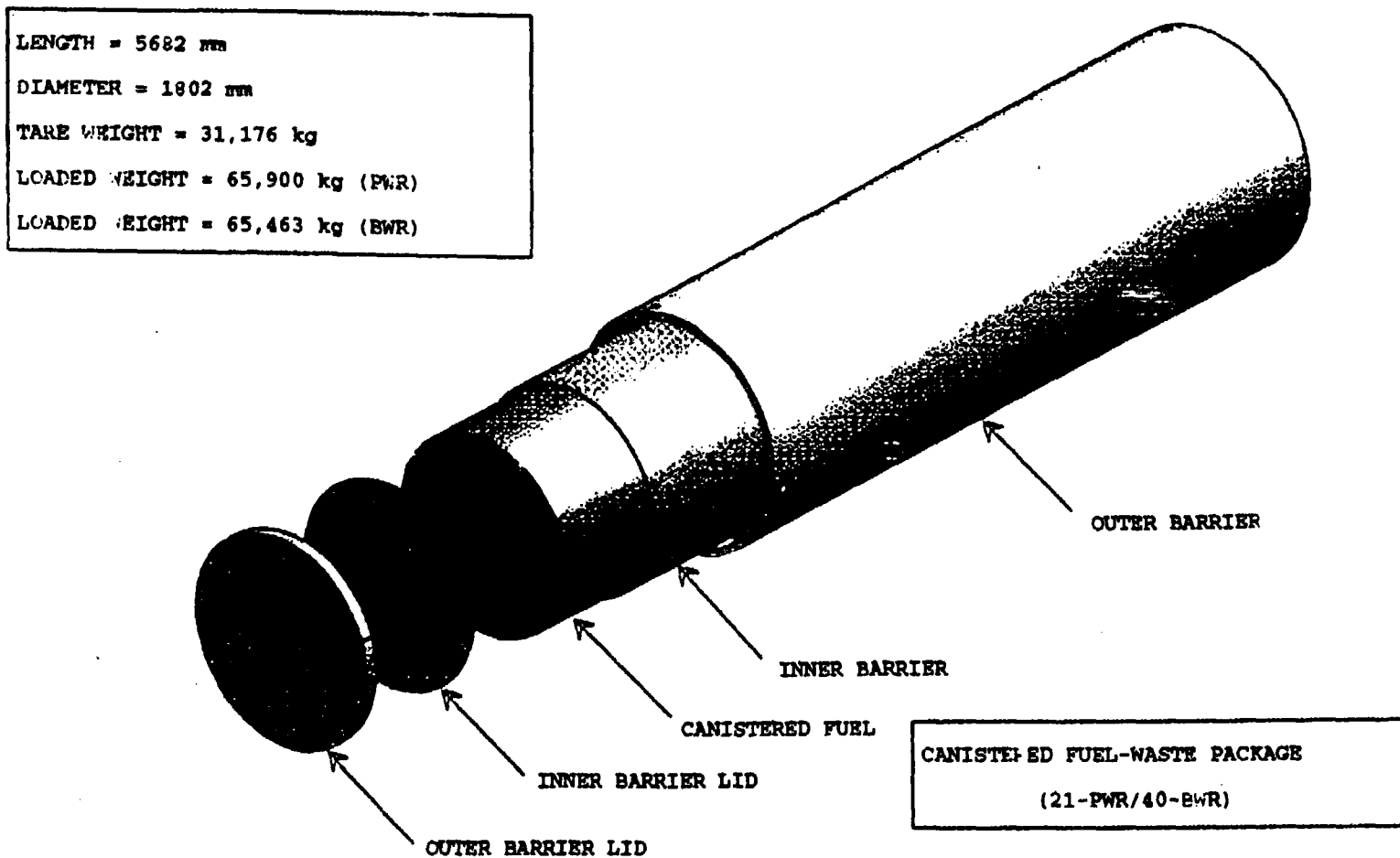
- The chemical composition, pH, and oxygen concentration of the condensed pore groundwater need to be modeled quantitatively in the presence of corrosion products. An example would be multi-phase, non-isothermal, and multi-dimensional mass transport modeling of the environment. Also, this modeling needs to include the effects of microbes, and cements. For this purpose, more details on the properties of microbes and cements need to be studied;
- More research needs to be done on the generation of colloids and on incrusting properties of corrosion products;
- Fast corrosion propagation needs to be quantified to assess accelerated formation of corrosion products. Such corrosion modes include localized corrosion, stress corrosion cracking, hydrogen embrittlement, and mechanical failure; and
- Detailed designs of waste packages and underground facilities, especially optional designs, should be provided.

## 6. CONCLUSIONS

In this report, we evaluated steels to be emplaced at the proposed Yucca Mountain repository. The evaluation focused on how much corrosion products are generated. Qualitative discussion on how corrosion products can affect the near-field environment was also made. In addition to steel overpacks, the sources of corrosion products include basket materials, multipurpose canisters (MPCs), pour canisters of HLW glass, and steel sets supporting drift walls. A design summary of these sources is presented. Based on uniform corrosion, most of these steels are likely to be corroded in 15,000 years. Approximately  $(3.6 - 4.5) \times 10^5$  MT of iron oxide will be generated from the corrosion of overpack within 10,000 years. With complete corrosion, MPCs will generate about  $(9.5 \times 10^4 - 1.2 \times 10^5)$  MT of iron oxide; basket materials will generate about  $(1.0 - 1.3) \times 10^5$  MT of iron oxide; pour canisters of HLW glass will generate approximately about  $(8.0 \times 10^3 - 1.0 \times 10^4)$  MT; and steel sets will generate about  $(2.1 - 2.6) \times 10^4$  MT. The corrosion products are expected to be incrustated under near-static conditions. However, unlike underground corrosion in soil, corrosion products may be sloughed off and colloids may be generated, with flowing or dripping groundwater. During corrosion, oxygen may be depleted in the near field. We also discussed how the corrosion environment may be altered by cement and microbes. With pitting corrosion, it is unclear how much concentrated and acidic pit chemistry would affect the overall chemistry outside of the pits.

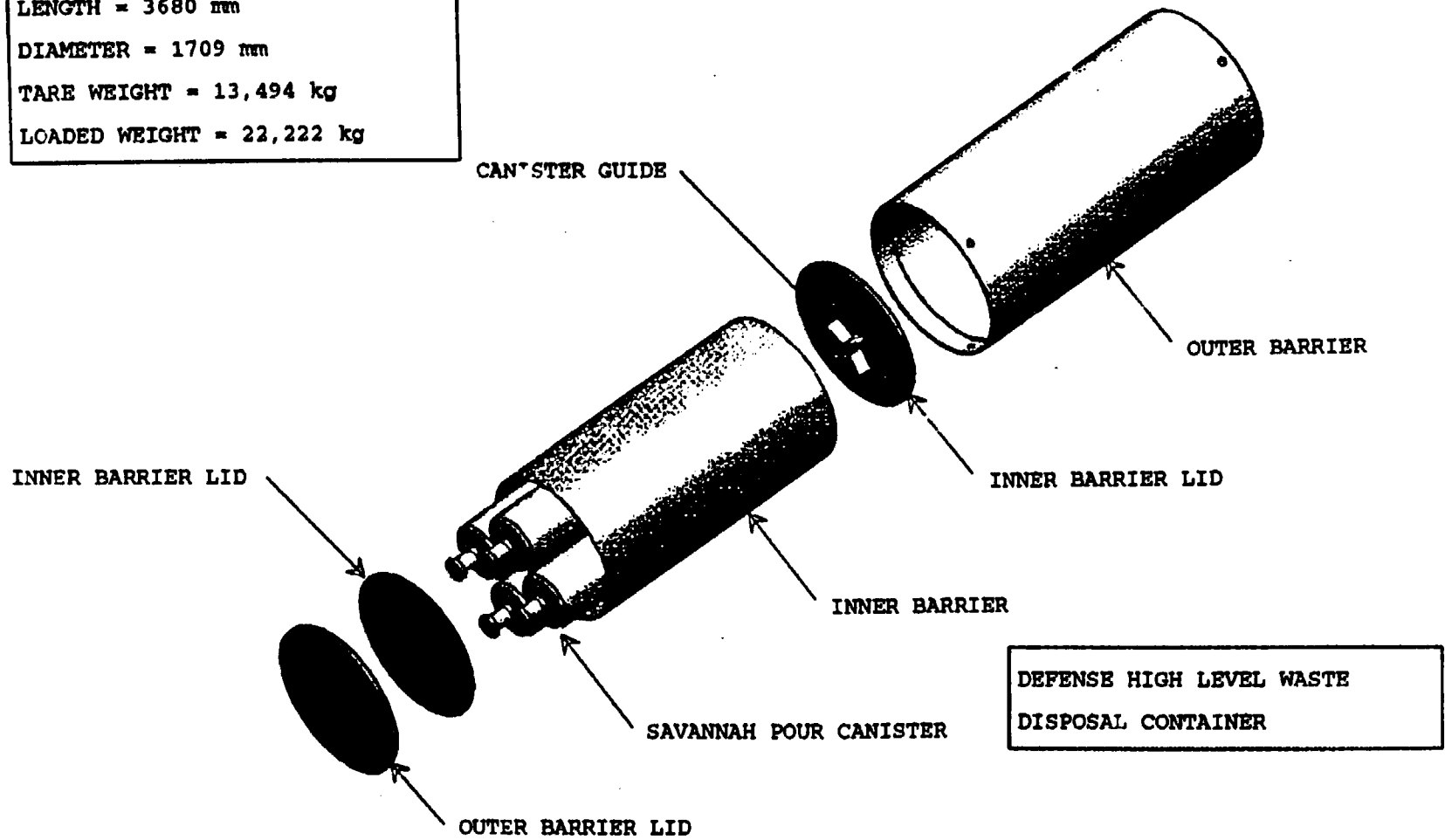
Figure 1. Waste Package Major Components [TRW Environmental Safety System, Inc., 1996]

(1-a). Canistered Spent Fuel Waste Package



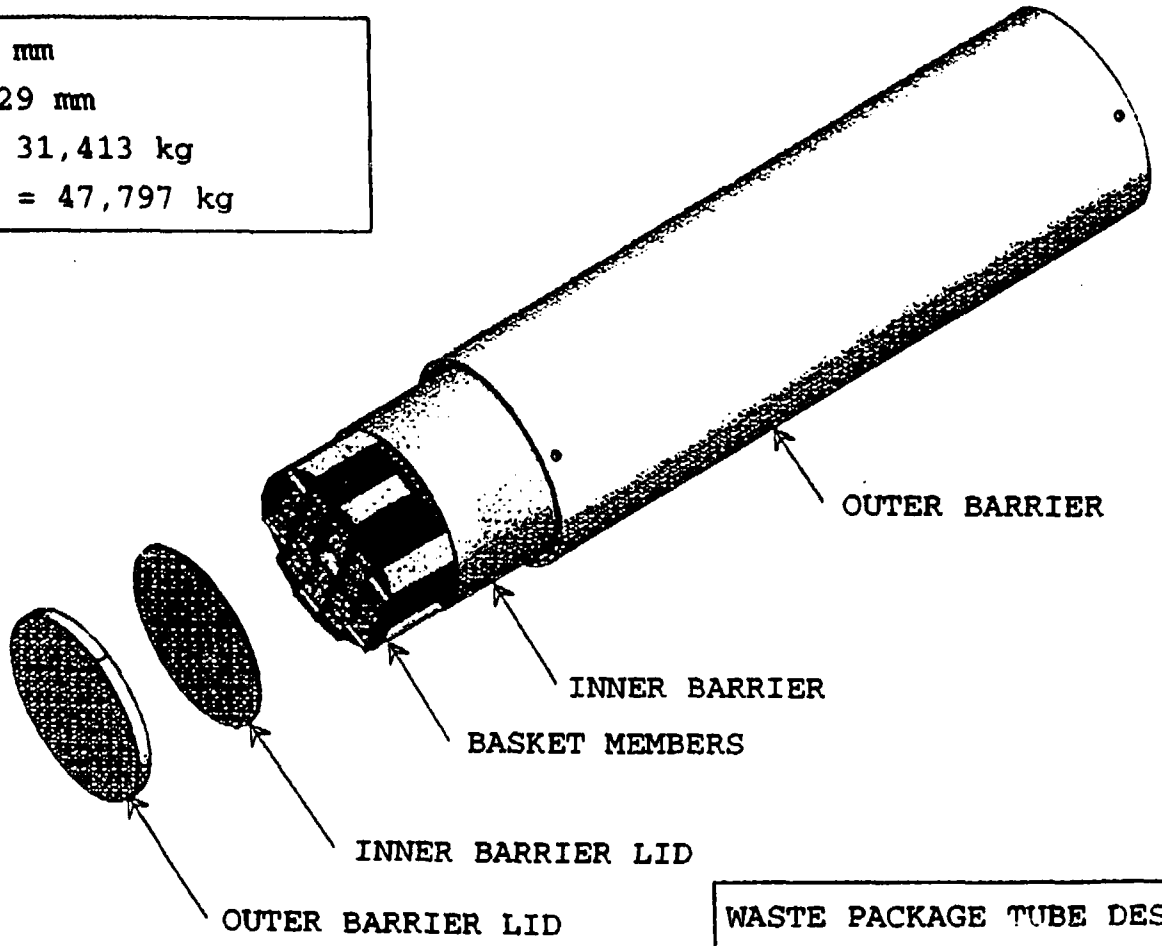
(1-b). High-Level Waste Glass Waste Package

LENGTH = 3680 mm  
DIAMETER = 1709 mm  
TARE WEIGHT = 13,494 kg  
LOADED WEIGHT = 22,222 kg



(1-c). Uncanistered Spent Fuel Waste Package

LENGTH = 5335 mm  
DIAMETER = 1629 mm  
TARE WEIGHT = 31,413 kg  
LOADED WEIGHT = 47,797 kg



WASTE PACKAGE TUBE DESIGN  
(21-PWR) MAJOR COMPONENTS

Figure 2. A Schematic of Basket Structure (1-a and 1-c) [TRW Environmental Safety System, Inc., 1996]

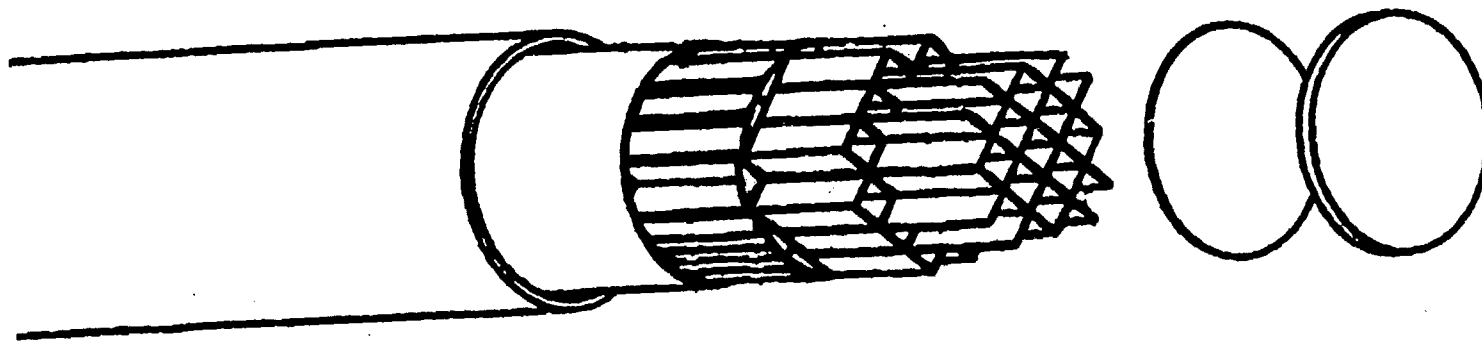


Figure 3. A Schematic of Steel Sets used in the ESF Design Construction [TRW Environmental Safety System, Inc., 1997]

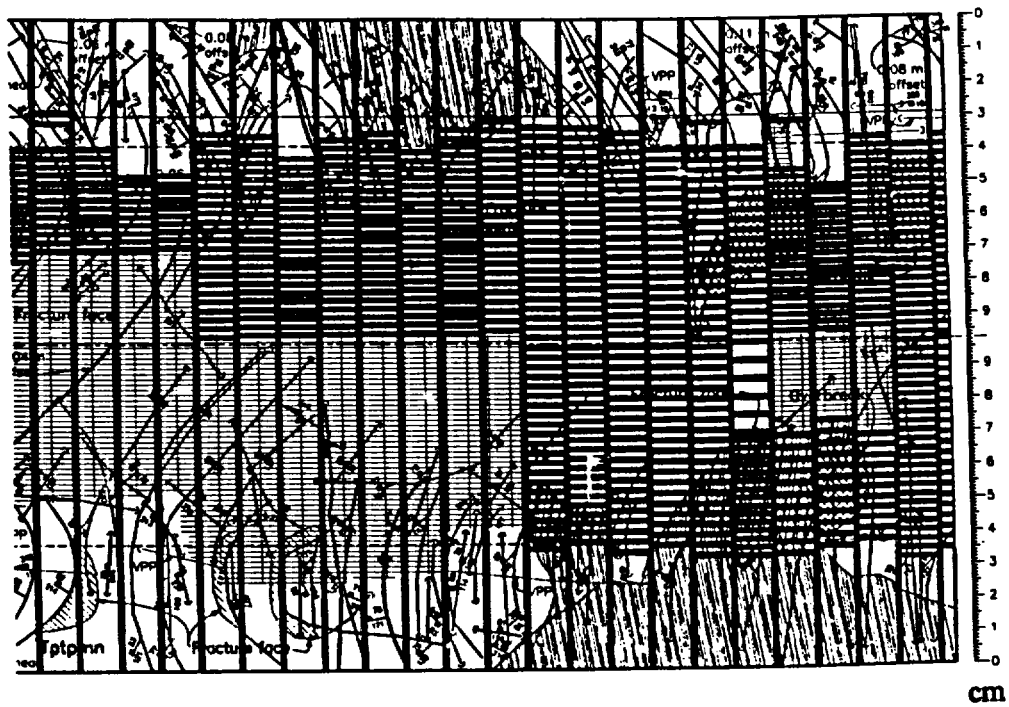
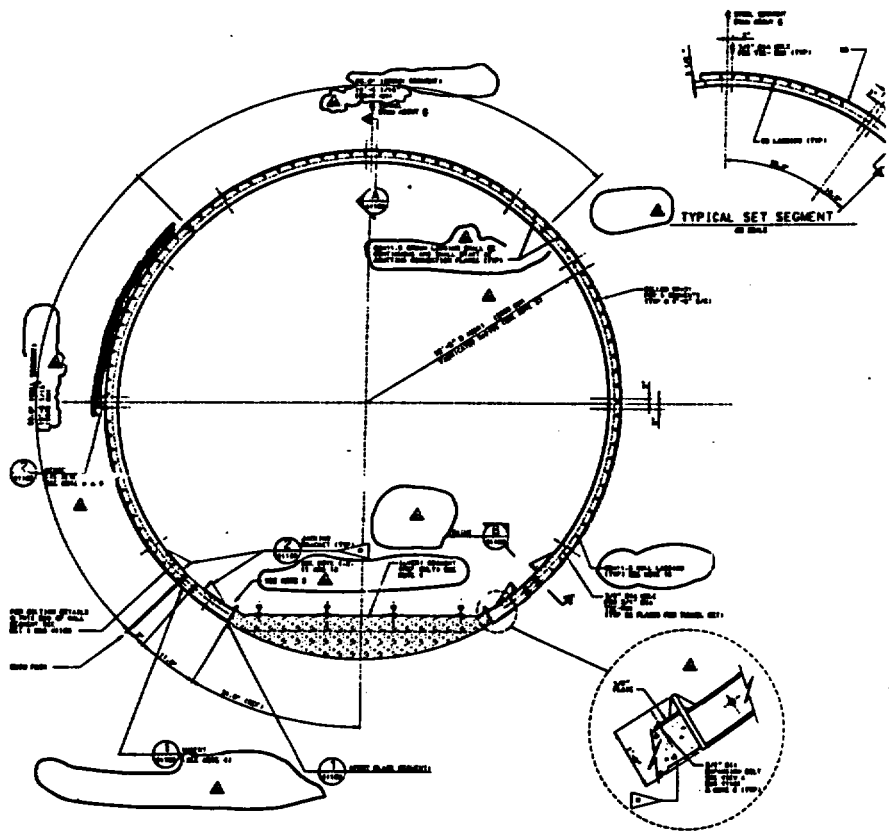


Figure 4. Predicted Temperature and Relative Humidity of Waste Package Surface [Wilder, 1996]

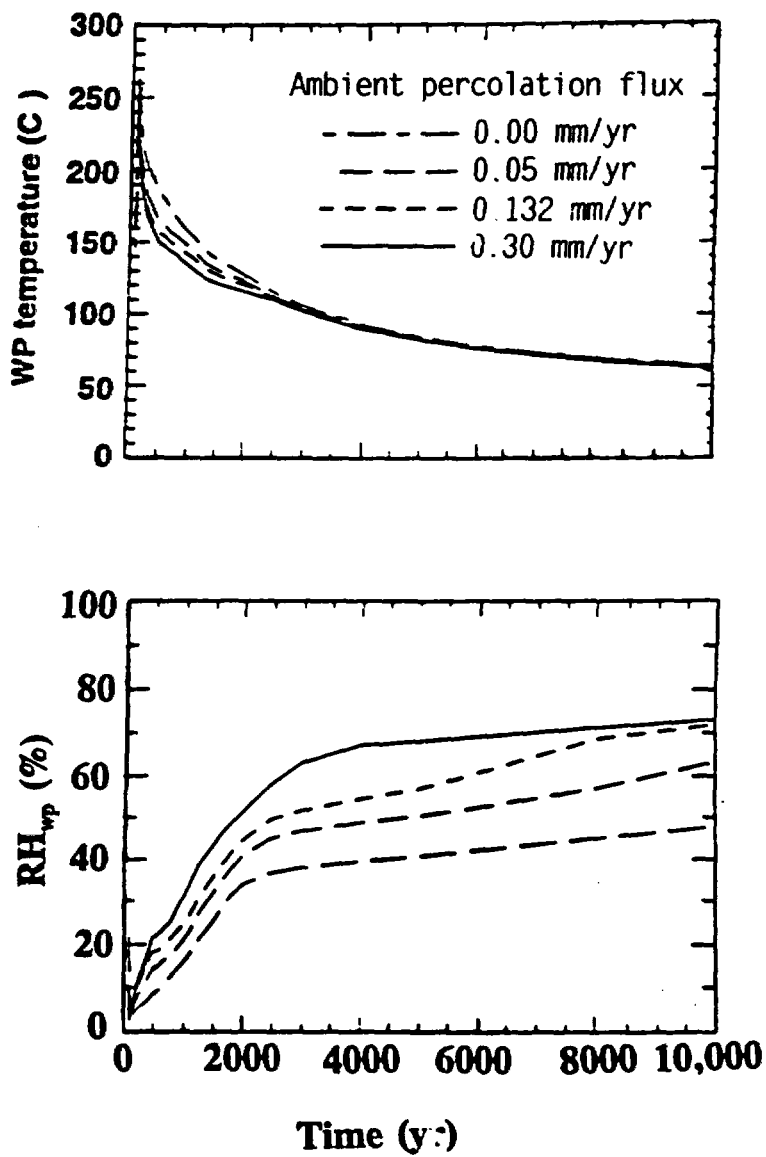


Figure 5. Model Prediction of (a) Aqueous General Corrosion and (b) Humid General Corrosion in DOE TSPA-95 [TRW Environmental Safety System Inc., 1995]

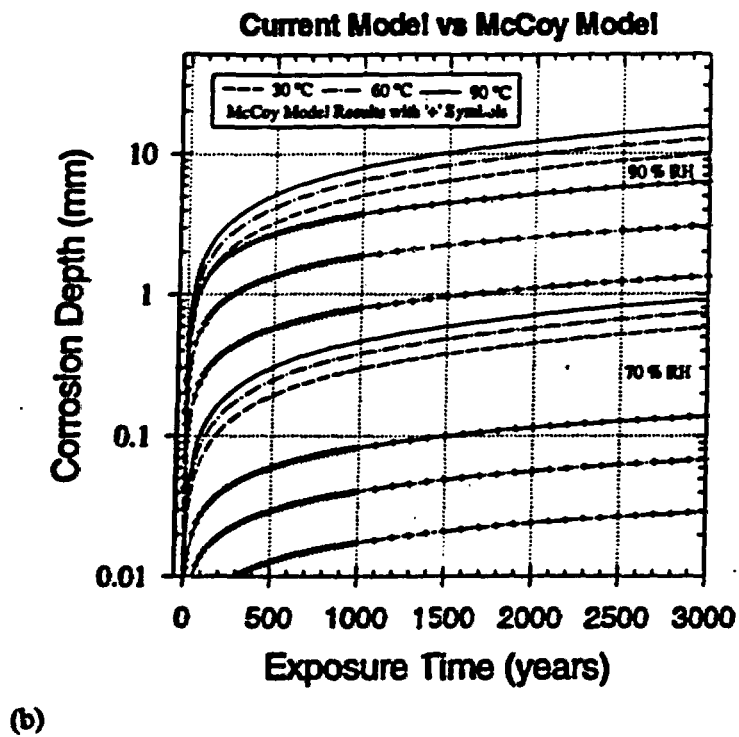
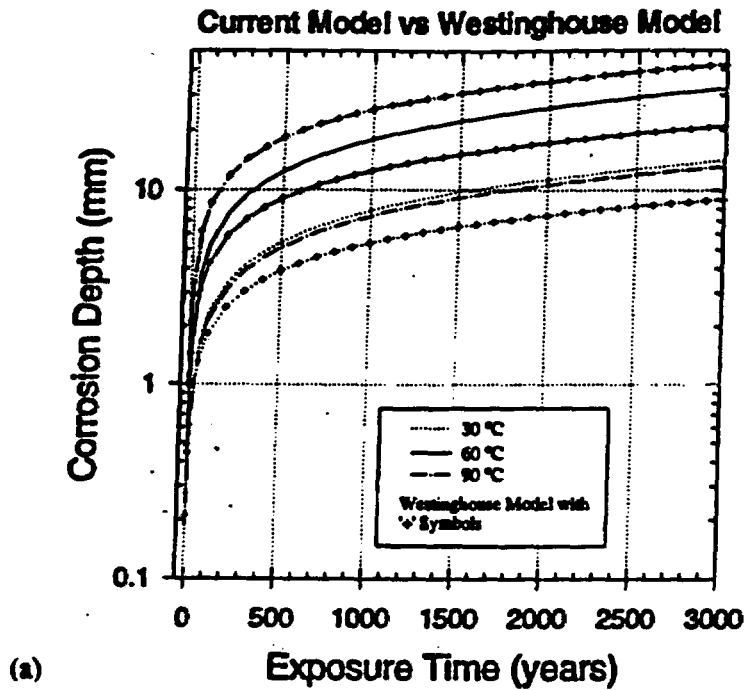


Figure 6. Potential-pH Diagrams for Iron and Water at Room Temperature [Pourbaix, 1974]

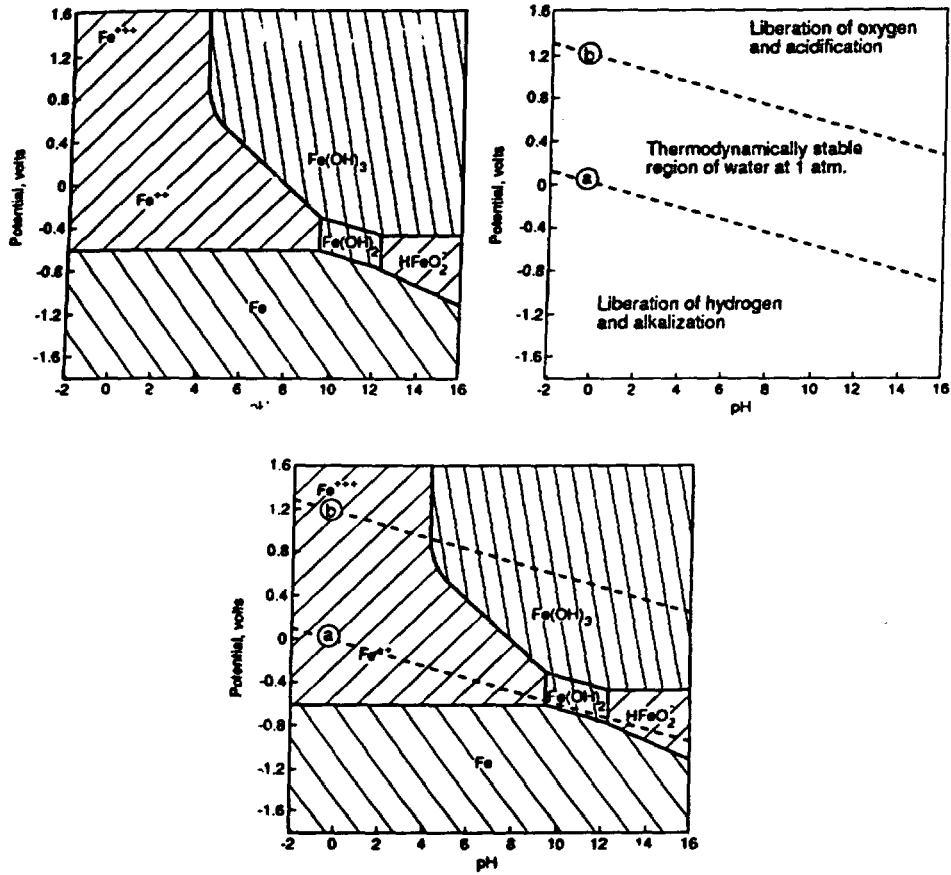


Figure 7. Corrosion of Buried Plain Carbon Steel after 14 Years of Exposure [Romanoff, 1957]

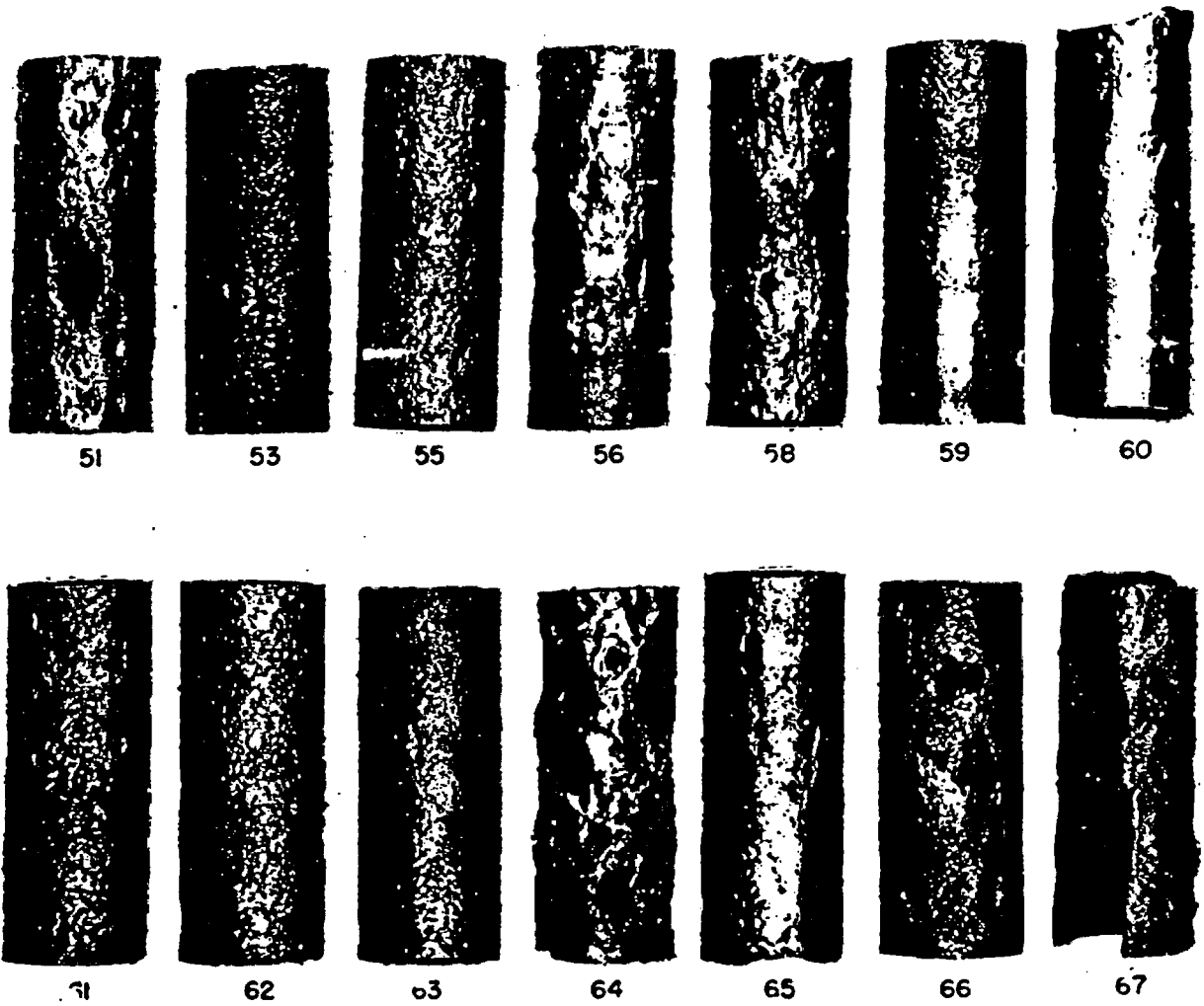


Figure 8. Chemistry inside Pit: (a) 18Cr-12Ni-2Mo-Ti Stainless and (b) Iron [Szklańska-Smiałowska, 1986]

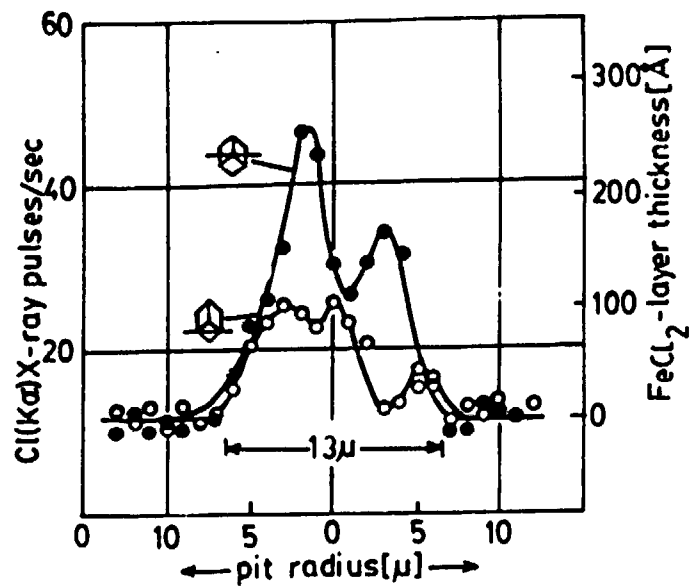
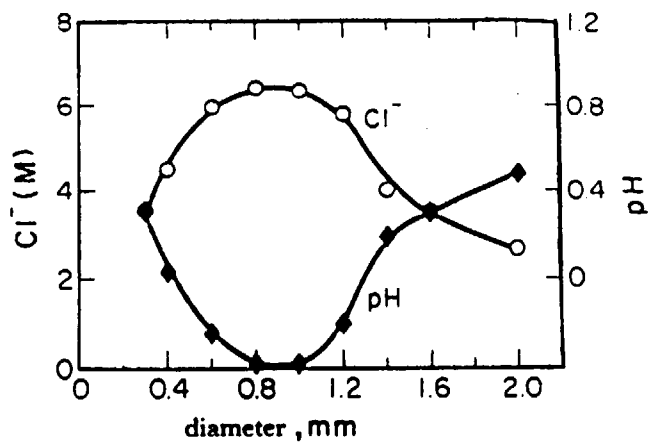


Table 1. Chemical Composition of Candidate Alloys [McCoy, 1996] for Overpack

1.1 Outer Layer

(extracted from American Society for Metals, 1978; and Cragolino, et al., 1996)

Steel	Element, wt. %						
	C	Mn	Si	Cr	Mo	S	P
A516 Grade 55	<2.4 <sup>a</sup>	0.55- 1.30 <sup>b</sup>	0.13- 0.45 <sup>b</sup>	-	-	0.04 max	0.035 max
A516 Grade 70	<0.3 1 <sup>c</sup>	0.85- 1.25	0.15- 0.30	-	-	0.04	0.035
A387 Grade 22	<0.1 7 <sup>a</sup>	0.25- 0.66 <sup>b</sup>	0.50 max	1.88- 2.62 <sup>b</sup>	0.85- 1.15 <sup>b</sup>	0.035 max	0.035 max

<sup>a</sup>: 100 to 200-mm-thick plate

<sup>b</sup>: Product analysis

<sup>c</sup>: Limiting values vary with the plate thickness

1.2 Inner Layer (extracted from American Society for Metals, 1980; and ASM International, 1992)

Alloy	Element, wt. %								
	Ni	Cr	Fe	Co	Mo	W	Nb	Mn	others
Alloy 625	bal	20.0-23.0	5.0	1.0	8.0-10.0		3.15-4.15*	0.50	0.40Ti 0.40Al 0.10C 0.50Si
Alloy C-22	bal	21.5	5.5	2.5	13.5	4.0		1.0	0.01C 0.1Si 0.3V
Alloy C-4	bal	14-18	3.00 max	2.00 max	14-17			1.00 max	0.70Ti 0.15C 0.08Si 0.04P 0.03S (max)

\*: Niobium plus Tantalum content

Table 2. Types of Stainless Steels to be Used for MPCs, Baskets, and Pour Canisters [Sridhar et al., 1994].

Steel	Element, wt. %						
	C,max	Cr	Cu	Fe	Mo	Ni	Others
304L	0.03	19.0	-	bal	-	10.0	Mn:2.0 max S:0.03 max P:0.045 max
316L	0.03	17.0	-	bal	-	12.0	Mn: 2.0 max S: 0.03 max Mn: 1.0 max

\* Borated stainless has a maximum 1.6 weight percent boron in a type close to 316 stainless steel [McCoy, 1996].

Table 3. Penetration Depth of Carbon Steel by Uniform Corrosion at Various Times Using a Constant Passive Current Calculated Using EBSPAC [Mohanty et al., 1996]

Year	1	10	$10^2$	$10^3$	$10^4$
P (cm)	$1.16 \times 10^{-3}$	$1.16 \times 10^{-2}$	$1.16 \times 10^{-1}$	1.16	$1.16 \times 10$

Table 4. Mass of Corrosion Products Generated as the Result of Complete Corrosion of Outer Overpacks

Corrosion product	Volume expansion	Density (g/cm <sup>3</sup> )	Weight per 11,000 container (MT)
Fe <sub>2</sub> O <sub>3</sub>	1.50	5.24	$3.70 \times 10^5$
Fe <sub>3</sub> O <sub>4</sub>	1.52	5.18	$3.57 \times 10^5$
Fe <sub>2</sub> O <sub>3</sub> •xH <sub>2</sub> O at x = 1	2.60	3.02	$4.53 \times 10^5$

\* Data on volume expansion and oxide density are from Handbook of Chemistry and Physics [CRC Press, 1975]. The density of carbon steel used was 7.77 g/cm<sup>3</sup> [Lynch, 1989].

Table 5. Mass of Corrosion Products Generated as the Result of Complete Corrosion of MPCs

Corrosion product	Volume expansion	Density (g/cm <sup>3</sup> )	Weight per 11,000 container (MT)
Fe <sub>2</sub> O <sub>3</sub>	1.50	5.24	9.80x10 <sup>4</sup>
Fe <sub>3</sub> O <sub>4</sub>	1.52	5.18	9.45x10 <sup>4</sup>
Fe <sub>2</sub> O <sub>3</sub> •xH <sub>2</sub> O at x=1	2.60	3.02	1.20x10 <sup>5</sup>

\* Data on volume expansion and density are from Handbook of Chemistry and Physics [CRC Press, 1975]. The density of carbon steel used was 7.77 g/cm<sup>3</sup> [Lynch, 1989].

Table 6. Mass of Corrosion Products Generated as the Result of Complete Corrosion of Basket Plates

Corrosion product	Volume expansion	Density (g/cm <sup>3</sup> )	Weight per 11,000 container (MT)
Fe <sub>2</sub> O <sub>3</sub>	1.50	5.24	1.06x10 <sup>5</sup>
Fe <sub>3</sub> O <sub>4</sub>	1.52	5.18	1.03x10 <sup>5</sup>
Fe <sub>2</sub> O <sub>3</sub> •xH <sub>2</sub> O at x=1	2.60	3.02	1.30x10 <sup>5</sup>

\* Data on volume expansion and density are from Handbook of Chemistry and Physics [CRC Press, 1975]

**Table 7. Mass of Corrosion Products Generated as the Result of Complete Corrosion of Pour Canisters**

Corrosion product	Volume expansion	Density (g/cm <sup>3</sup> )	Weight per 11,000 container (MT)
Fe <sub>2</sub> O <sub>3</sub>	1.50	5.24	8.24x10 <sup>3</sup>
Fe <sub>3</sub> O <sub>4</sub>	1.52	5.18	7.95x10 <sup>3</sup>
Fe <sub>2</sub> O <sub>3</sub> •xH <sub>2</sub> O at x=1	2.60	3.02	1.01x10 <sup>4</sup>

\* Data on volume expansion and density are from Handbook of Chemistry and Physics [CRC Press, 1975]

**Table 8. Mass of Corrosion Products Generated as the Result of Complete Corrosion of Steel Sets that could be Used as Drift Supports**

Corrosion product	Volume expansion	Density (g/cm <sup>3</sup> )	Weight (MT)
Fe <sub>2</sub> O <sub>3</sub>	1.50	5.24	2.15x10 <sup>4</sup>
Fe <sub>3</sub> O <sub>4</sub>	1.52	5.18	2.07x10 <sup>4</sup>
Fe <sub>2</sub> O <sub>3</sub> •xH <sub>2</sub> O at x=1	2.60	3.02	2.63x10 <sup>4</sup>

\* Data on volume expansion and density are from Handbook of Chemistry and Physics [CRC Press, 1975]

**Table 9. Pit Volume per Overpack with Various Pit Sizes and Pit Densities**

<b>Pit size (diameter, cm)</b>	<b>Pit density (per cm<sup>2</sup>)</b>	<b>Pit volume (cm<sup>3</sup>)</b>
$10^{-4}$	0.1	$3.15 \times 10^{-3}$
$3.2 \times 10^{-3}$	3.2	$1.03 \times 10^2$
$10^{-1}$	100	$3.15 \times 10^6$

\* The outer overpack volume is approximately  $3.03 \times 10^6$  cm<sup>3</sup>.

\* Cylindrical pit was assumed in calculations.

## 7. REFERENCES

Ahn, T. M., 1996a, Long-term Kinetic Effects and Colloid Formations in Dissolution of LWR Spent Fuels, NUREG-1564, U.S. Nuclear regulatory Commission, Washington, DC

Ahn, T. M., 1996b, Dry Oxidation and Fracture of LWR Spent Fuels, NUREG-1565, U.S. Nuclear Regulatory Commission, Washington, DC

Ahn, T. M., 1994, Long-Term C-14 Source Term for a High-Level Waste Repository, *Wast. Manag.*, 14, 393

ASM International, 1992, ASM Handbook, Vol.2, Materials Park, OH

American Society for Metals, 1987, 1980 and 1978, Metals Handbook, Ninth Edition, Vol.3, Metals Park, OH

Bates, J. K., J. P. Bradley, A. Teetsov, C. R. Bradley, and M. B. Brink, 1992, Colloid Formation During Waste Form Reaction, *Sci.*, 256, 649

Cragolino, G. A., H. K. Manaktala, and Y-M. Pan, 1996, Thermal Stability and Mechanical Properties of High-Level Radioactive Waste Container Materials: Assessment of Carbon and Low-Alloy Steels, CNWRA 96-004, Center for Nuclear Waste Regulatory Analyses, San Antonio, TX

CRC Press, 1975, Handbook of Chemistry and Physics, Cleveland, OH

Geesey, G, 1993, A Review of the Potential for Microbially Influenced Corrosion of High-Level Nuclear Waste Containers, CNWRA 93-014, Center for Nuclear Waste Regulatory Analyses, San Antonio, TX

Dzombak, D. A. and F. M. M. Morel, 1990, Surface Complexation Modeling: Hydrous ferric Oxide, John Wiley and Sons, New York, NY

Escalante, E., 1997, Personal Communication, National Institute of Standards and Technology, Gaithersburg, MD

Finn, P. A., J. K. Bates, J. C. Hoh, J. W. Emery, L. D. Hafenrichter, E. C. Buck, and M. Gong, 1994a, Elements Present in Leach Solutions from Unsaturated Spent Fuel Tests, *Mat. Res. Soc. Symp. Proc.*, 333, 399

Finn, P. A., M. Gong, J. K. Bates, J. W. Emery, and J. C. Hoh, 1994b, The Effect of Fuel Type in Unsaturated Spent Fuel Tests, Proceeding of the Fifth International High-Level Radioactive Waste Management Conference 2, 2, 1080, American Nuclear Society, La Grange Park, IL

Girvin, D. C., L. L. Ames, A. P. Schwab and J. E. McGarrah, 1991, Neptunium Adsorption on Synthetic Amorphous Iron Oxyhydroxide, *J. Col. and Int. Sci.*, 141, 67

Glassley, W. E., 1986, Reference Waste Package Environment Report, UCRL-53726, Lawrence

Livermore National Laboratory, Livermore, CA

Hunter, K. A., D. J. Hawke and L. K. Choo, 1988, Equilibrium Adsorption of Thorium by Metal Oxides in Marine Electrolytes, *Geo. et Cos. Act.*, 52, 627

Jones, D. A., 1992, Principles and Prevention of Corrosion, Macmillan Publishing Company. New York, NY

LaFlamme, B. D. and J. W. Murray, 1987, Solid/Solution Interaction: The Effect of Carbonate Alkalinity on Adsorbed Thorium, *Geo. et Cos. Act.*, 51, 243

Lichtner, P. C. and M. S. Seth, 1996, User's Manual for MULTIFLO: Part II - MULTIFLO 1.0 and GEM 1.0, Multicomponent - Multiphase Reactive Transport Model, CNWRA 96-010, Center for Nuclear Waste Regulatory Analyses, San Antonio, TX

Lynch, C. T., 1989, Practical Handbook of Materials Science, CRC Press, Inc., Boca Raton, FL

McCoy, J. K., 1997, Personal Communication, TRW Environmental Safety Systems, Inc., Las Vegas, NV

McCoy, J. K., 1996, Waste Package Materials Selection Analysis, BBA000000-01717-0200-00020, Rev.00, CRWMS/M&O, TRW Environmental Safety Systems, Inc., Las Vegas, NV

Manteufel, R. D., R. G. Baca, S. Mohanty, M. S. Jarzempa, R. W. Janetzke, S. A. Stothoff, C. B. Connor, G. A. Cragolino, A. H. Chowdhury, T. J. McCartin, and T. M. Ahn, 1997, Total-System Performance Assessment (TPA), Version 3.0 Code: Module Descriptions and User's Guide, Center for Nuclear Waste Regulatory Analyses, San Antonio, TX

Mohanty, S., G. A. Cragolino, T. Ahn, D. S. Dunn, P. C. Lichtner, R. D. Manteufel, and N. Sridhar, 1996, Engineered Barrier System Performance Assessment Code: EBSPAC Version 1.0  $\beta$ , Technical Description and User's Manual, CNWRA 96-011, Center for Nuclear Regulatory Analyses, San Antonio, TX

Murphy, W. M., 1991, Performance Assessment Perspectives with Reference to the Proposed Repository at Yucca Mountain, in Proceedings from the Technical Workshop on Near-Field Performance Assessment for High-Level Waste. Madrid, Spain, Swedish Nuclear Fuel and Waste Management Co., Stockholm, Sweden

Nolting, R., 1997, Personal Communication, TRW Environmental Safety Systems, Inc., Las Vegas, NV

Pourbaix, M., 1974, Atlas of Electrochemical Equilibria in Aqueous Solutions, CEDECOR, National Association of Corrosion Engineers, Houston, TX

Romanoff, M., 1957, Underground Corrosion, National Bureau of Standards Circular 579, National Bureau of Standards, Gaithersburg, MD

Sanchez, A. L., J. W. Murray and T. H. Sibley, 1985, The Adsorption of Plutonium IV and V on

Goethite, *Geo. et Cos. Act.*, 49, 2297

Savage, D., 1997, Review of the Potential Effects of Alkaline Plume Migration from a Cementitious Repository for Radioactive Waste: Implications for Performance assessment, R&D technical report P60, QuantiSci Ltd., Environment Agency, Bristol, Britain

Sridhar, N., G. A. Cragolino and D. S. Dunn, 1995, Experimental Investigations of Failure Processes of High-Level Nuclear Waste Container Materials, CNWRA 95-010, Center for Nuclear Waste Regulatory Analyses, San Antonio, TX

Sridhar, N., G. A. Cragolino, D. S. Dunn, and H. K. Manaktala, 1994, Review of Degradation Modes of Alternate Container Designs and Materials, CNWRA 94-010, Center for Nuclear Waste Regulatory Analyses, San Antonio, TX

Stockman, C., 1997, Personal Communication, Sandia National Laboratory, Albuquerque, NM

Szklarska-Smialowska, Z., 1986, Pitting Corrosion of Metals, National Association of Corrosion Engineers, Houston, TX

TRW Environmental Safety Systems Inc., 1997, ESF Design Drawing, partly available, Las Vegas, NV

TRW Environmental Safety Systems Inc., 1996, Mined Geologic Disposal System Advanced Conceptual Design Report, Volume III of IV, Engineered Barrier Segment/Waste Package, B00000000-01717-5705-00027, Rev.00, Las Vegas, NV

TRW Environmental Safety Systems Inc., 1995, Total System Performance Assessment - 1995: An Evaluation of the Potential Yucca Mountain Repository, B00000000-01717-2200-00136, Las Vegas, NV

U. S. Department of Energy, 1988, Site Characterization Plan: Yucca Mountain Site, Nevada Research and Development Area, Nevada, DOE/RW-0199, Office of Civilian Radioactive Waste Management, Washington, DC

Wilder, D. G., 1996, Preliminary Near-Field Environmental Report. Volume II: Near-Field and Altered-Zone Environment Report, Introduction and Chapter 1, UCRL-LA-124998, Lawrence Livermore National Laboratory, Livermore, CA

Wilder, D. G., 1993a, Preliminary Near-Field Environment Report. Vol. I: Technical Bases for EBS Design, UCRL-LR-107476, Lawrence Livermore National Laboratory, Livermore, CA

Wilder, D. G., 1993b, Preliminary Near-Field Environment Report. Vol.II: Scientific Overview of Near-Field Environment and Phenomena, UCRL-LR-107476, Lawrence Livermore National Laboratory, Livermore, CA

Yariv, S. and H. Cross, 1979, Geochemistry of Colloids Systems, Spring-Verlag, New York, NY